PIER C

(Received 27 April 2025, Accepted 17 June 2025, Scheduled 1 July 2025)

Performance Analysis of Electrical Impedance and Acoustic Tomography for Early Breast Cancer Detection

Annapoorani Ganesan[1] *, Vani Rajamanickam[1], and Vaishali Durgamahanthi[2]

[1] *Department of Electronics and Communication Engineering, Faculty of Engineering and Technology SRM Institute of Science and Technology, Ramapuram Campus, Chennai 600089, Tamil Nadu, India*
[2] *Department of Electronics and Communication Engineering, Faculty of Engineering and Technology SRM Institute of Science and Technology, Vadapalani Campus, Chennai 600026, Tamil Nadu, India*

ABSTRACT: Breast cancer is considered one of the major cancers among women. Early identification of breast cancer is essential for improving treatment outcomes, necessitating the application of accurate, noninvasive imaging methods. This paper presents a comparative evaluation of Electrical Impedance Tomography (EIT) and Ultrasound Tomography (UST) for breast tumor diagnosis, employing a simulated multilayer breast model. The forward problem, which entails the determination of electrical conductivity and acoustic pressure distribution, was addressed through finite element analysis utilizing COMSOL Multiphysics software. The inverse problem of EIT was solved using Total Variation regularization with Primal-Dual Interior Point Method (TV-PDIPM), and that of ultrasound by employing attenuation-weighted bilinear interpolation to effectively resolve propagation losses through tissue layers, subsequently leading to segmentation. The images reconstructed and segmented from both modalities were subjected to quantitative evaluation employing metrics such as Accuracy, Sensitivity, Specificity, and Relative Image Error. The findings indicate that both approaches offer complementary information regarding the tumor, presenting distinct advantages based on tissue characteristics and image clarity.

1. INTRODUCTION

Among women, breast cancer accounted for most cases in 157 out of 185 nations, and globally, breast cancer claimed 670,000 lives in the year 2022 [1]. Early diagnosis of breast cancer increases survival rates and treatment outcomes. While conventional imaging techniques like mammography, MRI, and ultrasound are widely used, they have limitations in terms of cost, radiation exposure, and accessibility [2]. Alternative imaging techniques, such as Thermography, Optical Tomography, and Electrical Impedance Tomography (EIT), have been investigated due to their non-ionizing and economical characteristics.

EIT is a portable, noninvasive imaging method that may be used for continuous monitoring due to its affordability [3, 4]. Biomedical EIT primarily relies on alterations in tissue-related properties, specifically the electrical characteristics of biological tissues. EIT leverages variations in tissue conductivity to distinguish between healthy and malignant regions, making it a viable diagnostic and monitoring tool in clinical applications [5]. Administering a controlled current to the human tissue and monitoring the resultant voltage at the periphery allows the inference of internal conductivity distributions [6, 7]. A smaller-scale experiment by [8] used 80 electrodes to recreate a cancer model constituting 0.1% of the breast model's volume. In [9], an EIT-IC (Integrated Circuit) featuring a broad bandwidth of 10 MHz was developed to detect small-sized tumours measuring up to 0.5 cm. A rotational EIT technique was proposed to resolve two tumours separated by 1.5 cm without increasing electrode complexity [10]. Apart from 2D, several 3D EIT systems have been proposed in recent years. Furthermore, various 3D EIT systems have emerged, including a multi-circle planar sensor for high-resolution micro-imaging [11], a reconstruction approach using sparsity and median filtering [12], and a 3D technique based on dimensional grey wolf optimization (DGWO) to mitigate shape and position sensitivity [13].

Ultrasound Tomography (UST) is employed to reconstruct the acoustic impedance distribution of the target region employing the principles of acoustic propagation. In contrast to EIT, UST is responsive to interfaces between various biological tissues and has an excellent spatial resolution in the center region [14]. UST cannot identify micro-calcifications and has restricted spatial resolution; nonetheless, it enhances overall sensitivity and specificity, achieving rates of 76% and 84%, respectively [15]. Recent years have seen a notable increase in interest surrounding dual-modality techniques, primarily because they offer the potential for complementary insights from different types of imaging. The widespread use of ultrasound studies in the healthcare sector can be attributed to its accessibility and cost-effectiveness as a noninvasive imaging method [16]. In [17], a novel pixel fusion technique utilizing fuzzy logic for Electrical Capacitance Tomography (ECT) and UST images has been proposed. In [18], threshold effect was addressed, and the meta-analysis indicates that the Ultrasound (US) and Mammography (MMG) have comparable diagnostic performance. Based on individual lesions, however, US was found to have a higher diagnostic accuracy than MMG.

* Corresponding author: Annapoorani Ganesan (annapoog2@srmist.edu.in).

This work presents a novel methodologically coherent performance evaluation of UST and EIT using a common multi-layered breast model. Utilizing identical performance metrics such as sensitivity, specificity, accuracy, and Relative Image Error (RIE), this study allows a consistent comparison that emphasizes the complementary diagnostic advantages of both modalities, laying a basis for future frameworks based on multimodal fusion. Improvements in metric values are evident due to the implementation of advanced reconstruction and segmentation algorithms. The following sections are structured in this manner: Section 2 details the forward and inverse modelling of EIT and UST systems. Section 3 provides the results along with a comparative analysis, while Section 4 wraps up the paper with concluding remarks.

2. METHODOLOGY

2.1. Mathematical Model of EIT and UST

The forward problem of Electrical Impedance Tomography (EIT) is defined by three fundamental equations: Dirichlet boundary conditions, Neumann boundary conditions, and Maxwell's equations. According to Maxwell's system of equations [18],

$$-\nabla\left(\sigma\nabla V\right)=0 \tag{1}$$

where σ is the conductivity distribution, and V is the scalar potential distribution inside the field. In this study, the complete electrode model (CEM) [19] is utilized to address the EIT forward problem through the finite element method.

$$u+z_1\sigma\frac{\partial U}{\partial V}=V_1 \quad \text{On} \quad E_l, \quad l=1,2,L \tag{2}$$

$$\int_{E_l}\sigma\frac{\partial U}{\partial V}\cdot\partial\Omega=I_l \quad \text{Where} \quad I_l=1,2,L \tag{3}$$

$$\sigma\frac{\partial U}{\partial V}=0 \quad \text{on} \quad \frac{\Gamma}{\bigcup_{l=1}^{L}E_l} \quad E_l=1,2,L \tag{4}$$

In the context of the UST forward problem, examine a one-dimensional medium characterized by the absence of sources and lossless properties. The mass density of the body is denoted as $p_0(x)$, while the body pressure is represented by p_0. The total pressure (p_T) in a propagating pressure wave is expressed as

$$p_T\left(x,t\right)=p_0+p(xt) \tag{5}$$

The wave equation governing the acoustic field is expressed as follows:

$$\frac{1}{\rho_0 c_s^2}\frac{\partial^2 p}{\partial t^2}=\nabla\cdot\left(\frac{1}{\rho_0}\nabla_p\right) \tag{6}$$

Consider the Lorentz force $\vec{q}$. The wave equation is modified to

$$\frac{1}{\rho_0 c_s^2}\frac{\partial^2 p}{\partial t^2}=\nabla\cdot(\frac{1}{\rho_0}\left(\nabla_p-\vec{q}\right) \tag{7}$$

We utilized COMSOL Multiphysics 6.0 due to its exceptional accuracy and robust physics-based modelling features to tackle the forward problem. This software environment facilitates the simulation and resolution of finite element analysis challenges. The solution to the forward problem included multiple physics modules, such as electric currents, solid mechanics, and pressure acoustics for the frequency domain study. A two-dimensional circular shape breast prototype has been created, having a diameter of 7 cm, incorporating multiple layers that simulate an authentic breast structure, as illustrated in Figure 1.

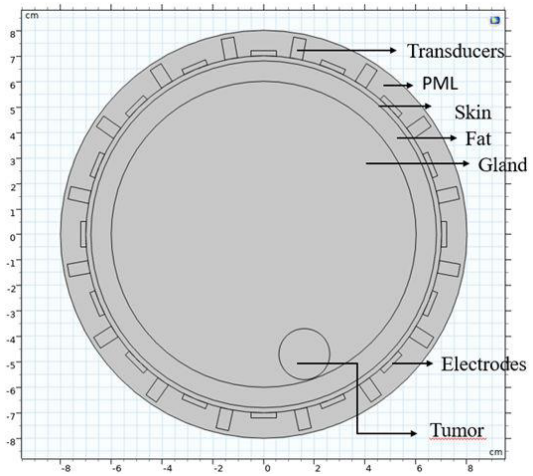

FIGURE 1. Geometry of breast phantom.

2.2. Implementation of the Forward Problem Utilizing COMSOL Multiphysics

In the context of EIT experiments, a total of 16 electrodes composed of Ag/AgCl were utilized to deliver current to the tissue and to record the resulting voltage responses. An adjacent electrode configuration is utilized, with a 1 mA alternating current supplied to electrode 1 using a boundary current source and ground to electrode 2 at a frequency of 50 kHz. Table 1 presents the material properties [20, 21] utilized in the modelling process. A triangular finer mesh is utilized in the EIT forward problem to enhance accuracy and expedite simulation processes.

TABLE 1. Dielectric properties used in COMSOL for EIT.

Layers	Electrical Conductivity (S/m)	Relative Permittivity
Skin	2.73E-4	1.13E+3
Fat	2.49E-2	1.18E+2
Gland	5.34E-1	4.02E+3
Malignant Tumor	1.12	60

Alongside the electrode responsible for current conduction, the voltage distribution across the remaining components of the electrode pairing is documented. The medical device standard 60601-1 is adhered to, as demonstrated in the development of early breast cancer EIT-IC [22]. The experiment was conducted repeatedly until each electrode operated as a current source. After documenting the voltage measurements in the evaluation table, they were stored in a ".xlsx" file. The boundary current

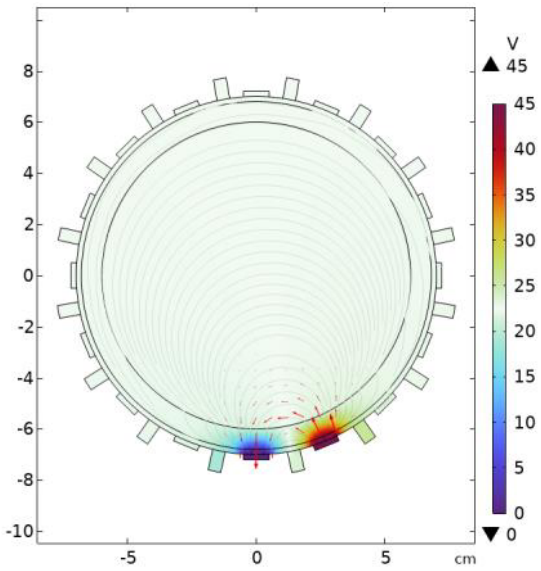

FIGURE 2. EIT-based voltage distribution in a homogeneous medium.

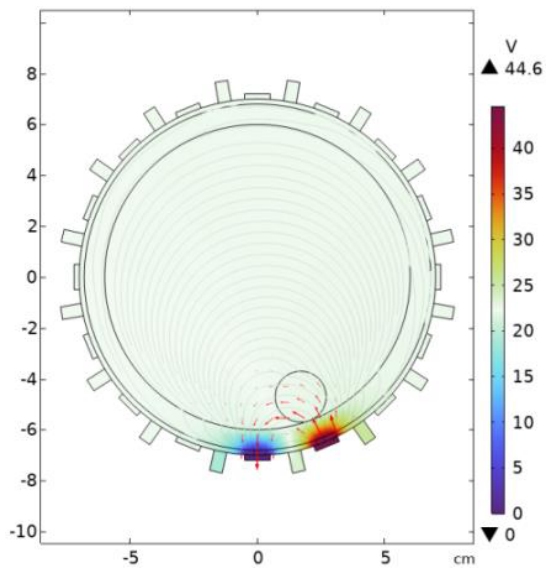

FIGURE 3. EIT-based voltage distribution in a heterogeneous medium.

source is governed by

$$n \cdot (J_1 - J_2) = Q_{j \cdot s} \tag{8}$$

The Pressure Acoustics frequency domain module, part of the Acoustic Module, outlines the acoustic properties, including speed of sound and density, pertinent to breast ultrasound modelling and its boundary conditions within the context of ultrasound measurements. Equation (16) is the equation for ultrasonic waves in a lossless medium for acoustic pressure. COMSOL handled the Helmholtz equation, expressed as a

$$\nabla \left(-\frac{1}{\rho_c} \left(\nabla p_t - q_d \right) \right) - \frac{k_{eq}^2 p_t}{\rho_c} = Q_m \tag{9}$$

$$k_{eq}^2 = \left(\frac{\omega}{c_c} \right)^2 - k_z^2 \tag{10}$$

As ρ denotes the medium's density, q_d and Q_m represent the monopole and dipole sources; k_{eq} denotes the associated wave number over the waveform velocity cc in the fluid; k_z signifies the out-of-plane wave number; and ρ_c pertains to the density of the medium. As the ultrasonic wave travels through a multiphase medium distribution, various attenuation mechanisms — such as diffusion, scattering, and absorption — take place at the interfaces of the different media. Consequently, the ultrasonic transducer at the receiving end captures the sound pressure signal that has been attenuated [23]. This configuration employs 16 ultrasound PZT-4 transducers arranged in an alternating ring pattern, utilizing a free triangular mesh having a maximum element size of $\lambda/6$ [24]. A Perfectly Matched Layer (PML) is given as an outer boundary that absorbs outgoing ultrasound waves. A pressure of 100 kPa is applied to the first transducer using the pressure boundary condition, and the corresponding acoustic pressure is recorded from the other transducers acting as receivers. The experiment proceeds until all transducers function as transmitters. A study in the frequency domain is conducted at 1 MHz, with the corresponding acoustic pressure recorded and organized in a table. The acoustic pressure distribution is shown in Figure 3.

2.3. Modelling the Inverse Problem for EIT and UST

Using boundary measurements to recreate the internal characteristics of breast tissue is the goal of the inverse problem in Electrical Impedance Tomography (EIT) and Ultrasound Tomography (UST). In the context of breast cancer detection, this section outlines the reconstruction methods used for EIT and UST.

The open-source EIDORS (Electrical Impedance Tomography and Diffuse Optical Tomography Reconstruction Software) toolbox in MATLAB was employed for the inverse problem in EIT. Due to the pronounced susceptibility of EIT to noise and modeling inaccuracies, Total Variation (TV) regularization is utilized to preserve discrete conductivity gradients while mitigating artifacts [25, 26]. The following is the formulation of the reconstruction problem.

$$\hat{\sigma} = \arg\min \|V_m - V_c\|^2 + \lambda \int |\nabla \sigma| \, dx \tag{11}$$

λ is the regularization parameter that controls smoothness, and V_m and V_c are the measured and calculated boundary voltages. The reconstructed images are segmented using the Fuzzy C Means Segmentation algorithm, which eliminates the need for manual seeding and performs effectively even with noisy EIT images [27]. Fuzzy C Means (FCM) permits data points to be associated with different clusters, exhibiting differing levels of affiliation. This is particularly advantageous in medical image processing, where tissue borders may be indistinct or confluent. The clustering procedure in FCM is accomplished by reducing the subsequent objective function:

$$J_{m=\sum_{i=1}^{N}\sum_{j=1}^{C} \mu_{ij}^m \|x_i - c_j\|^2} \tag{12}$$

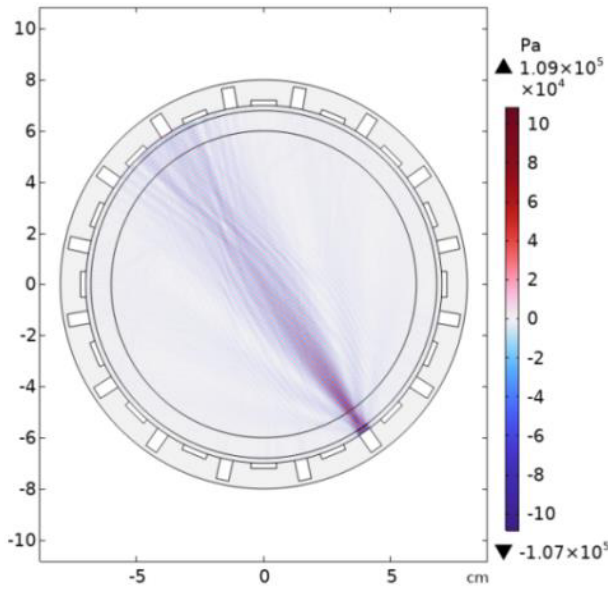

FIGURE 4. Acoustic pressure distribution in a homogeneous medium.

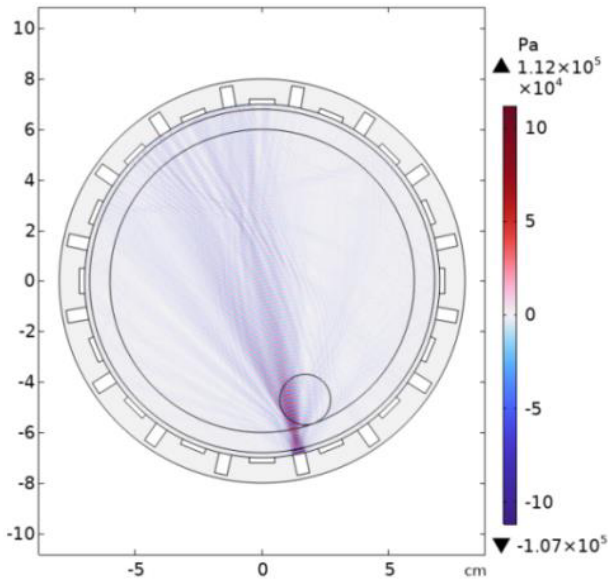

FIGURE 5. Acoustic pressure distribution in a heterogeneous medium.

where N represents the total count of pixels, C the total number of clusters, μ_{ij} the degree of membership, c_j the center of the jth cluster, and m the fuzzy parameter.

The inverse problem of reconstructing the spatial acoustic pressure distribution for UST was executed completely in MATLAB, utilizing attenuation-weighted bilinear interpolation. To prepare for inversion, pressure data from COMSOL simulations is interpolated into a uniform 2D grid (512×512). Following rectification, the data is normalized after the removal of diagonal (self-interaction) terms. Using known tissue-specific attenuation constants (in dB/m) for areas such as skin, fat, glandular tissue, and tumors, a spatial attenuation map is produced. To properly address tissue-dependent losses, this map applies an exponential decay factor to the pressure data. K-means clustering is used to segment the normalized reconstructed image using $k = 3$ clusters. The cluster with the highest intensity most likely represents the tumor. This segmentation separates regions into the background, normal tissue, and probable tumor locations. To the output, morphological techniques, such as area-based filtering and linked component analysis are used.

3. RESULTS AND DISCUSSIONS

3.1. Forward Problem Simulation

Figure 2 depicts the potential distribution within a homogeneous tissue of a 7 cm radius, consisting of multiple layers, as simulated with COMSOL Multiphysics software. The voltage distribution across the breast phantom is uniform. Figure 3 illustrates a tumor with a radius of 1 cm, embedded within a breast-mimicking phantom. A reduced value in potential distribution indicates the presence of a malignant tumor, which demonstrates higher conductivity than normal breast tissue.

Under the Pressure Acoustics physics interface in COMSOL, a 100 kPa pressure signal is transmitted into the breast phantom using a PZT4 ultrasonic transducer. The breast phantom for UST uses the same construction as the EIT. A frequency domain analysis was conducted at 1 MHz, and Figure 4 displays the matching acoustic pressure from the receiver. As seen in Figure 5, the existence of a tumor is indicated by a higher acoustic pressure from the receiver following anomaly insertion. Both EIT and UST underwent the same studies, and the outcomes were recorded and saved in an Excel file for inverse problem-solving.

3.2. Image Reconstruction and tumor Segmentation

The inverse of EIT entails the reconstruction of the internal conductivity distribution of the breast based on measurements of boundary voltages. This study utilized a total variation (TV) regularization-based inverse solver to improve edge preservation and reduce noise in the reconstructed images. The reconstruction process utilized the Primal-Dual Interior Point Method (PDIPM), recognized for its efficient convergence in non-smooth optimization scenarios. This image is preprocessed to remove noise and artifacts and given as input to the segmentation algorithm, which segments the tumor region as shown in Figure 6(a).

A reconstruction method based on attenuation-weighted bilinear interpolation was used to solve the inverse problem in UST. This novelty will improve the localization of acoustic impedance variations, making tumor detection more precise. COMSOL simulations' raw pressure data was given as input to the algorithm along with transducer positions. An exponential attenuation model, which was based on known attenuation coefficients for skin, fat, glandular tissue, and tumor locations, was used to account for acoustic losses.

Unsupervised K-means clustering with three clusters was used to segment the normalized image after attenuation correction, signifying background, normal tissue, and malignancy as shown in Figure 6(b). To measure the size and position of the tumor, a centroid and bounding box were calculated as represented in Figure 7 for the final location detected.

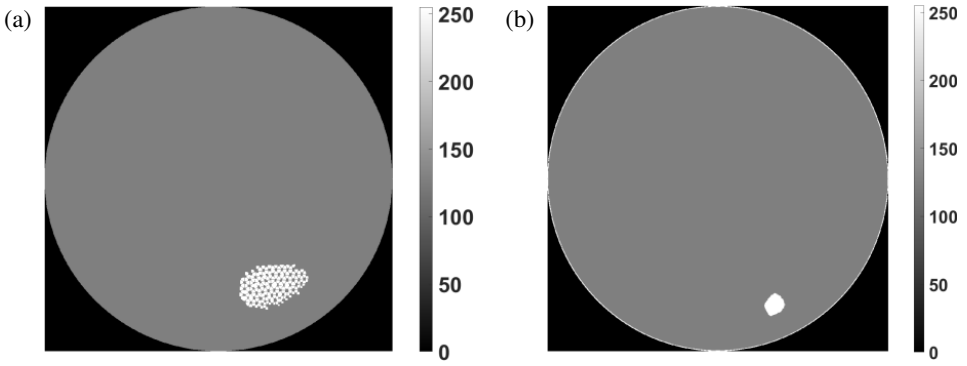

FIGURE 6. (a) Segmented region highlighting the tumor in EIT. (b) Segmented region highlighting the tumor in Ultrasound Tomography (UST).

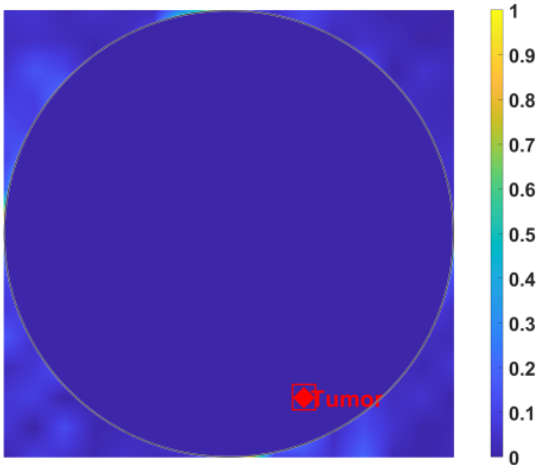

FIGURE 7. Tumor bounding box.

The performance metrics of EIT and UST are shown in Figures 8 and 9 as evaluation criteria. The performance of EIT is largely influenced by the differences in electrical conductivity between healthy and malignant tissues, with malignant tissues exhibiting higher values. In UST, acoustic pressure waves engage with tissue boundaries, rendering this modality especially responsive to structural variations. Malignant tumors exhibit greater attenuation compared to normal tissues. The tomography's performance in differentiating tumor and non-tumor regions was evaluated using accuracy, sensitivity, and specificity metrics. Relative image error (RIE) in percentage shows the difference between the reconstructed (I_r) and ground truth image (I_g).

1. Accuracy $= \frac{TP+TN}{TP+TN+FP+FN}$

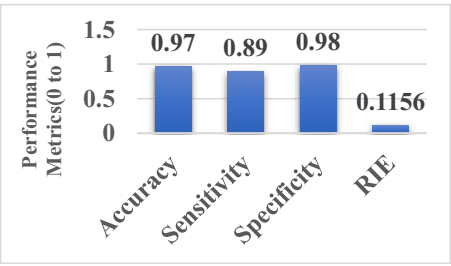

FIGURE 8. Performance metrics of Electrical impedance tomography.

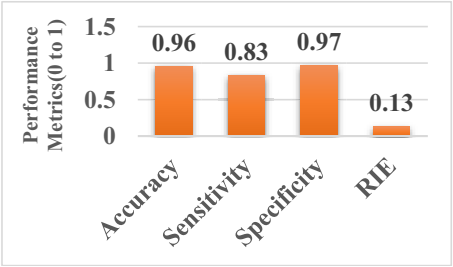

FIGURE 9. Performance metrics of ultrasound tomography.

2. Sensitivity $= \frac{TP}{TP+FN+\epsilon}$
3. Specificity $= \frac{TN}{TN+FP+\epsilon}$
4. RIE$= \frac{\|I_r-I_g\|}{I_g}$

4. CONCLUSION

This paper has presented a performance analysis of two non-invasive methods for breast cancer detection, specifically EIT and UST. It demonstrates the correlation and complementary information obtained through a comparative assessment of individually reconstructed images. The forward modelling was conducted in a realistic multilayered breast tissue phantom utilizing a combination of 16 electrodes and 16 PZT transducers, implemented through COMSOL Multiphysics software. A novel reconstruction algorithm was developed in MATLAB utilizing TV_PDIPM with total variation in the prior, followed by advanced fuzzy c-means segmentation that works well even for noisy EIT images. We have also focused on attenuation-corrected acoustic pressure interpolation for ultrasound applications. The simulation results were assessed utilizing clinically relevant performance metrics, indicating that both modalities can yield valuable images for tumor identification and localization. However, the current work focuses exclusively on simulation data. In the upcoming study, we aim to expand this research by validating the results using physical breast phantoms, ensuring their practical relevance. Additionally, we strive to incorporate advanced image fusion techniques to merge the structural details offered by ultrasound with the functional conductivity contrast derived from EIT, thereby enhancing diagnostic accuracy and clinical relevance. The noninvasive and low-cost characteristics of these modalities provide a

viable option for standard breast cancer detection, particularly in remote locations, for pregnant women, and for individuals with denser breast tissue.

REFERENCES

[1] World Health Organization, "Breast cancer key facts," https://www.who.int/news-room/fact-sheets/detail/breast-cancer, Mar. 2024.

[2] Zeeshan, M., B. Salam, Q. S. B. Khalid, S. Alam, and R. Sayani, "Diagnostic accuracy of digital mammography in the detection of breast cancer," *Cureus*, Vol. 10, No. 4, e2448, 2018.

[3] Annapoorani, G. and D. Vaishali, "Design and analysis of forward problem of electrical impedance tomography for breast cancer screening," in *AIP Conference Proceedings*, Vol. 3159, No. 1, 020019, 2025.

[4] Akhtari-Zavare, M. and L. A. Latiff, "Electrical impedance tomography as a primary screening technique for breast cancer detection," *Asian Pacific Journal of Cancer Prevention*, Vol. 16, No. 14, 5595–5597, 2015.

[5] Al Ahmad, M., Z. A. Natour, F. Mustafa, and T. A. Rizvi, "Electrical characterization of normal and cancer cells," *IEEE Access*, Vol. 6, 25 979–25 986, 2018.

[6] Wu, J., P. Wang, Y. Tang, H. Liu, H. Wang, W. Zhang, Y. Zhang, L. Chen, Z. Xu, and X. Yao, "A new method to rapidly identify benign and malignant breast lumps through bioelectrical impedance spectroscopy," *Medical Physics*, Vol. 46, No. 5, 2522–2525, 2019.

[7] Ye, G., K. H. Lim, R. T. G. Jr., G. A. Ybarra, W. T. Joines, and Q. H. Liu, "3D EIT for breast cancer imaging: System, measurements, and reconstruction," *Microwave and Optical Technology Letters*, Vol. 50, No. 12, 3261–3271, 2008.

[8] Hong, S., K. Lee, U. Ha, H. Kim, Y. Lee, Y. Kim, and H.-J. Yoo, "A 4.9 mΩ-sensitivity mobile electrical impedance tomography IC for early breast-cancer detection system," *IEEE Journal of Solid-State Circuits*, Vol. 50, No. 1, 245–257, 2014.

[9] Lee, J., S. Gweon, K. Lee, S. Um, K.-R. Lee, and H.-J. Yoo, "A 9.6-mW/Ch 10-MHz wide-bandwidth electrical impedance tomography IC with accurate phase compensation for early breast cancer detection," *IEEE Journal of Solid-State Circuits*, Vol. 56, No. 3, 887–898, 2020.

[10] Murphy, E. K., A. Mahara, and R. J. Halter, "Absolute reconstructions using rotational electrical impedance tomography for breast cancer imaging," *IEEE Transactions on Medical Imaging*, Vol. 36, No. 4, 892–903, Apr. 2017.

[11] Yang, L., H. Wu, K. Liu, B. Chen, S. Huang, and J. Yao, "A multicircle planar electrical impedance tomography sensor for 3-D miniature imaging," *IEEE Sensors Journal*, Vol. 23, No. 9, 9697–9706, May 2023.

[12] Yin, X., Y. Yang, J. Jia, and C. Tan, "3D image reconstruction on a miniature planar EIT sensor using sparsity with median filter," in *2017 IEEE SENSORS*, 1–3, Glasgow, UK, Oct. 2017.

[13] He, J., Z. Hong, X. Sun, Q. Deng, M. Zhu, C. Zhu, K. Liu, B. Sun, and J. Yao, "Three-dimensional image reconstruction of breast tumor by electrical impedance tomography based on dimensional grey wolf optimization algorithm," *IEEE Transactions on Instrumentation and Measurement*, Vol. 74, 4504310, 2025.

[14] Duric, N., P. Littrup, L. Poulo, A. Babkin, R. Pevzner, E. Holsapple, O. Rama, and C. Glide, "Detection of breast cancer with ultrasound tomography: First results with the Computed Ultrasound Risk Evaluation (CURE) prototype," *Medical Physics*, Vol. 34, No. 2, 773–785, 2007.

[15] Chen, H.-l., J.-q. Zhou, Q. Chen, and Y.-c. Deng, "Comparison of the sensitivity of mammography, ultrasound, magnetic resonance imaging and combinations of these imaging modalities for the detection of small (≤2 cm) breast cancer," *Medicine*, Vol. 100, No. 26, e26531, Jul. 2021.

[16] Mercado, K. P. E., "Developing high-frequency quantitative ultrasound techniques to characterize three-dimensional engineered tissues," Ph.D. dissertation, University of Rochester, Rochester, NY, USA, 2015.

[17] Pusppanathan, J., R. A. Rahim, F. A. Phang, E. J. Mohamad, N. M. N. Ayob, M. H. F. Rahiman, and C. K. Seong, "Single-plane dual-modality tomography for multiphase flow imaging by integrating electrical capacitance and ultrasonic sensors," *IEEE Sensors Journal*, Vol. 17, No. 19, 6368–6377, 2017.

[18] Tadesse, G. F., E. M. Tegaw, and E. K. Abdisa, "Diagnostic performance of mammography and ultrasound in breast cancer: A systematic review and meta-analysis," *Journal of Ultrasound*, Vol. 26, No. 2, 355–367, 2023.

[19] Somersalo, E., M. Cheney, and D. Isaacson, "Existence and uniqueness for electrode models for electric current computed tomography," *SIAM Journal on Applied Mathematics*, Vol. 52, No. 4, 1023–1040, 1992.

[20] Halter, R. J., T. Zhou, P. M. Meaney, A. Hartov, R. J. Barth, K. M. Rosenkranz, W. A. Wells, C. A. Kogel, A. Borsic, E. J. Rizzo, and K. D. Paulsen, "The correlation of in vivo and ex vivo tissue dielectric properties to validate electromagnetic breast imaging: Initial clinical experience," *Physiological Measurement*, Vol. 30, No. 6, S121, 2009.

[21] Fernández-Aranzamendi, E. G., P. R. Castillo-Araníbar, E. G. S. R. Castillo, B. S. Oller, L. Ventura-Zaa, G. Eguiluz-Rodriguez, V. González-Posadas, and D. Segovia-Vargas, "Dielectric characterization of ex-vivo breast tissues: Differentiation of tumor types through permittivity measurements," *Cancers*, Vol. 16, No. 4, 793, 2024.

[22] Davidson, J. L., P. Wright, S. T. Ahsan, R. L. Robinson, C. J. D. Pomfrett, and H. McCann, "fEITER — a new EIT instrument for functional brain imaging," in *Journal of Physics: Conference Series*, Vol. 224, No. 1, 012025, 2010.

[23] Li, F., Y. Liu, Z. Qiao, and Y. Li, "Convolutional attention network for electrical/ultrasound dual-modal fusion 2-D image reconstruction," *IEEE Transactions on Instrumentation and Measurement*, Vol. 73, 4503013, 2024.

[24] Annapoorani, G., R. Vani, and D. Vaishali, "Multi-modal finite element modelling for enhanced breast cancer detection using electrical impedance tomography and ultrasound tomography," in *2023 Second International Conference on Advances in Computational Intelligence and Communication (ICACIC)*, 1–6, Puducherry, India, Dec. 2023.

[25] Wu, Y., Y. Jiang, H. Ji, B. Wang, and Z. Huang, "A joint image reconstruction method for capacitively coupled electrical impedance tomography," *IEEE Transactions on Instrumentation and Measurement*, Vol. 73, 1–13, 2023.

[26] Ganesan, A. and V. Durgamahanthi, "Non-invasive breast cancer detection using electrical impedance tomography: Design, analysis and comparison of reconstruction algorithms," *Traitement du Signal*, Vol. 40, No. 6, 2809–2817, 2023.

[27] Sakai, K., P. N. Darma, P. A. Sejati, R. Wicaksono, H. Hayashi, and M. Takei, "Gastric functional monitoring by gastric electrical impedance tomography (gEIT) suit with dual-step fuzzy clustering," *Scientific Reports*, Vol. 13, No. 1, 514, 2023.